

## Development of Pressure Drop Model for the Compartment in Reactor Containment\*

Cheol Park, In-ho Song and Un Chul Lee

Seoul National University

(Received April 11, 1986)

### 격납용기내 구분방사이의 압력강하 계산모델 개발

박 철 · 송인호 · 이은철

서울대학교

(1986. 4. 11 접수)

#### Abstract

Full scale HDR containment experiment series pointed out that the previous containment analysis models have a number of shortcomings. One of them is on the calculational model of short term (0~2sec) pressure difference. The pressure differences between subcompartments are dependent on the flow rate, fluid density, head loss coefficient, and flow area ratio. It, however, is not known that any of them is largely attributed to the disagreement of pressure difference between the measured and the calculated values. In this study, the head loss coefficients are expressed with another form to improve the analytic model. The pressure and the pressure difference are evaluated by using COMPARE code with new correlation, and the results show better agreements with experimental values for V. 42 test, but overestimate the measured values for V. 43 and underestimate for V. 44.

#### 요 약

실제 발전소규모의 HDR 격납용기 실험에서 기존의 격납용기 해석모델에 많은 문제점들이 있다는 것이 밝혀졌는데, 그 중의 하나가 단기(0~2초) 압력 차이 계산이다. 격납용기의 각 구분방 사이의 압력차이는 질량 흐름율, 유체밀도, 마찰상실계수, 흐름면적비 등에 의존하는데, 각 요소가 압력 차이의 실험값과 계산값의 불일치에 어느 정도의 영향을 주는가는 정확하게 알려져 있지 않다. 본 연구에서는 기존의 해석모델을 개선하기 위해 지금까지 상수로 간주되어 온 마찰상실계수를 압력과 압력차이 등의 함수로 제시되었다. COMPARE 코드로 수정된 모델을 사용하여 HDR 실험에 대한 압력과 압력차이가 계산되었는데 V. 42 실험값에서는 측정치와 잘 맞고, V. 43의 측정치 보다는 높게, V. 44 실험값보다는 조금 낮은 결과를 보였다.

#### I. Introduction

In nuclear power plant, the containment must

be designed to withstand the consequences of any postulated accidents including LOCA (loss-of-coolant accident) to ensure that radioactivity does not leak to the environment. Hence pressure,

\* This research is supported by Korean Trade Scholarship Foundation

temperature and loadings on equipments in the containment should be known to evaluate the consequences of postulated accidents. Homogeneous containment analysis model gave rise to some problems such as local pressure buildup due to complex geometry inside containment and its large scale. So it requires the subcompartment analysis in which the states of each subcompartment are calculated. The previous models, however, are based on the results obtained from the experiments performed under simple geometry and restricted conditional variables. In order to solve these problems, Battelle-Frankfurt containment experiment which succeeded CVTR experiment was performed in Germany with large scale to improve the previous analytic models in 1975. But the application of these data was limited owing to its 1/10 scale of the actual nuclear power plant. Hence full scale Heiss-Dampf Reaktor (HDR) containment experiments were performed for more practical understanding. These tests revealed that several modeling defects still remained. In previous model for calculation of short term pressure difference, the flow resistance was not assumed precisely due to the complex geometry, droplets deposition and effective flow density. The pressure differences between subcompartments are dependent on the flow rate, fluid density, head loss coefficient, and flow area ratio. It is not known that any of them is dominantly attributed to the disagreement of pressure difference between the experimental and the calculated values. Up to date, we have simplified the head loss coefficient,  $K$ , as some constants depending on vent geometry, flow velocity and area ratio. But it may not be constant because the head loss coefficient has relation to the flow rate and the pressure difference which are rapidly varying during accidents transient. If head loss coefficient is not precisely defined, it may lead to the inaccurate pressure difference in the subcompartment anal-

ysis. So in this study, key parameters to influence the head loss coefficient are examined.

## II. Problem Descriptions

### II.1 General Flow Descriptions

The flow geometry between subcompartments is appropriately modeled in figure 1;

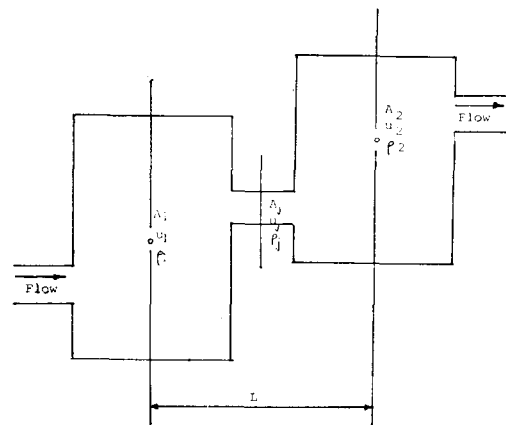


Fig. 1. Simplified Flow Geometry

For the above flow geometry we can obtain the following equation from momentum balance,

$$\frac{L}{A_j} \frac{d\dot{m}_j}{dt} = P_1 - P_2 - K \frac{\dot{m}_j^2}{2\rho_j A_j^2} \quad (1)$$

or,

$$I \frac{d\dot{m}_j}{dt} = \Delta P - \frac{K}{A_j^2} \frac{\dot{m}_j^2}{2\rho_j} \quad (2)$$

where,

$I = L/A_j$  (junction inertia) and

$\rho_j$  = effective flowing density.

In the derivation of equation (2), it is assumed that the pressure gradient can act only through available opening  $A_j$ . The time dependent momentum balance equation (2) is influenced by four parameters;

- i) vent flow area ( $A_j$ ),
- ii) effective path length ( $L$ ),
- iii) head loss coefficient ( $K$ ),
- iv) effective density ( $\rho_j$ ).

In other words, experimental pressure differences can be generated analytically not by a

unique set but by a whole range of combinations of the noted parameters. Thus these parameters can be specified within a physically plausible range.

(1) Total head loss coefficient,  $K$

As the head loss coefficient represents the effective flow resistance between two points at which pressures are measured or calculated, it is considered as one of the most important parameters. So far, in the subcompartment analysis,  $K$  has been evaluated by the flow resistances of the flow opening itself. For example, in short channels the friction is usually negligible and the resistance is restricted to entrance and exit losses. The maximum exit head losses have been evaluated theoretically as  $I$  and the entrance losses which depend on the entrance shape and area ratio have the maximum values of  $0.5 \sim 0.6$  according to Idel'chik. Therefore  $K$  can have a maximum value of 1.6. But the velocity of the flow opening calculated by such model is usually lower than the real velocity. Impact on the  $K$  within this narrow range on  $\Delta P$  values is small. Thus, openings would be also interpreted as a sharp-edged orifices. Because the fluid has to be accelerated to effectively higher velocities through a "vena contracta" produced by the momentum change imposed by a sharp-edged orifices. This interpretation broadens the range of justifiable  $K$  values,  $0 \sim 2.7$ . But it is shown that this range is not able to accommodate the resistances of the flow geometries within the HDR containment. Generally the flow between the subcompartments is regarded as compressible flow in subcompartment analysis. This is the case for the short term transients with high quality fluid after break. If the fluid is expansible, compressibility is important on the down stream side of the flow openings because it permits radial as well as longitudinal expansion to take place. And it can influence flow density and vena contracta and can change the head

loss coefficient to about 20%. Therefore the compressibility of the fluid is added to the determination of flow coefficient through orifices for the compressible flow.

(2) Effective path length for fluid acceleration,  $L$

Up to now,  $L$  has been evaluated according to prescription developed for channel flow. But it is not appropriate for the geometry as shown in Figure 1. It is because only some portions of the atmosphere which is in the vicinity of flow junction must be accelerated in large containment zones. Therefore,  $L$  is dependent on the flow junction area,  $A$ , and not on the total cross-sectional area of the control volume.

(3) Effective density of the flowing fluid,  $\rho$

This parameter is important as much as head loss coefficient because calculated  $P$  can be influenced largely by the effective fluid density. This is dependent on the two effects, the heat transfer rate into structures ( $\dot{q}_{st}$ ) and the effective acceleration factor of the suspended liquid ( $\xi$ ). Heat transfer to structures produces water condensation. Since the condensed steam is not accelerated to flow out of the break subcompartment, condensation may increase the density of a subcompartment atmosphere. So the density in the momentum equation (2) should include only that fraction of suspended water which is accelerated to the same velocity as the steam.

## II. 2 Characteristics of V. 42, V. 43 and V. 44 tests

The major differences between the three tests are the liquid level within the pressure vessel because these altered the blowdown energy and duration. The level are 2.8m, 6m and 9.2m for V. 42, V. 43 and V. 44 tests, respectively. The blowdown energy and mass can influence the average density in subcompartments and alter the pressure buildup. The second difference is the flow geometry. In figure 2, a schematic of

the flow junctions between subcompartments is shown. Volume 1 is a break compartment. Junctions connecting break compartment with adjacent compartments are classified into three grades according to the complexity. Geometries of junction 3 and junction 4 are complex. Other junctions have relatively simple openings. V. 42 and V. 43 tests are performed with same geometry, but for V. 44 test net area gain of  $0.74\text{m}^2$  is made from the area changes in the ceiling and simple openings. It can alter the flow characteristics (potential for momentum changes), but may not influence much. Impingement plate distances from the break nozzle are considered as another factor. The distances are 1m, 1m and 1.5m for tests V. 42, V. 43 and V. 44, respectively. This plays an important role in determining the extent of break flow distribution, which can change the acceleration of break compartment atmosphere and the momentum of flowing steam-water mixture.

### III. Modeling

#### 1) Compartment Modeling

HDR facility consists of many subcompartments. The detailed descriptions of each subcompartment are listed in references 12-14. Subcompartments with similar physical conditions can be lumped as a node for short computing time within the allowable ranges. For this study, a 14 compartment model is used and schematic representation is shown in Figure 2.

#### 2) Vent Modeling

All vents can be considered to be in the one of the following four categories;

- i) convergent or divergent nozzle
- ii) sharp-edged orifice
- iii) short channel
- iv) other miscellaneous vents

It is important to fit a given vent into one

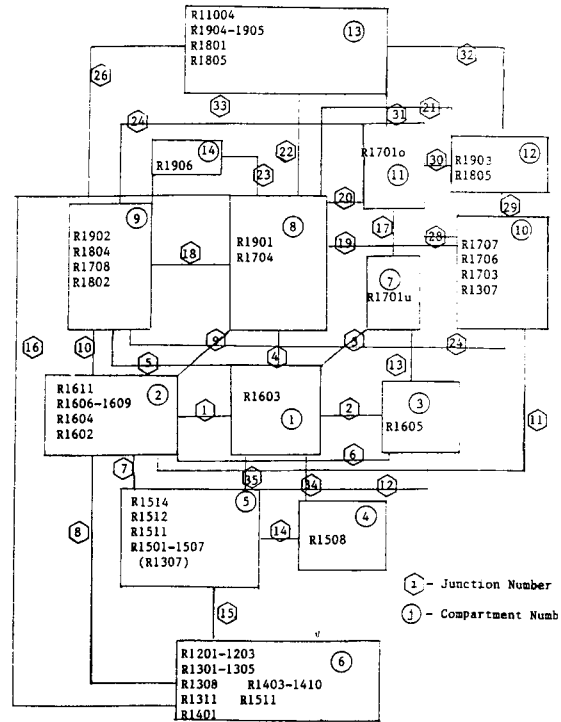


Fig. 2. Schematic of Compartments and Junctions For HDR Compartment Model

of these categories and to select an appropriate head loss coefficients. It is shown that the measured pressure difference in the HDR experiment describes the driving potential for most of the fluid leaving the break compartment. Thus, in this study all vents are considered as sharp-edged orifices and the head loss coefficient is expressed as one of the followings;

$$K = \frac{1}{\left(-0.16 \frac{\Delta P}{P} + 0.608\right)^2} \quad (3)$$

or

$$K = \frac{(1-\gamma)(1-\gamma^2)}{\left(-0.16 \frac{\Delta P}{P} + 0.608\right)^2} \quad (4)$$

or

$$K = 2.7 (1-\gamma)(1-\gamma^2) \quad (5)$$

where  $\gamma$  is the area ratio between junctions.

Equation (5), which approximates the head loss coefficient equation by Idel'chik, is used for the comparison with equation (3) and (4).

#### IV. Analysis

##### 1) Computational Procedures

A quasi-static method of analysis where the properties are assumed constant at a given time step is used to solve the equations in COMPARE code. So that, the analysis is performed as following procedures;

At a given time step,

- i) Specified mass and energy through the blowdown is added to the break compartment.
- ii) New thermodynamic conditions in the subcompartments are calculated as follows;
  - a. Calculate the specific volume of vapor.
  - b. Determine whether the flow is two-phase or superheated by comparing the saturated internal energy with the actual internal energy.

$$U_{sat} = C_p M_a (T_{sat} - 491.67) + M_{su} u_{sat}$$

- c. Calculate internal energy at  $T_{as}$

for two-phase,

$$U_{as} = M_a C_v (T_{as} - 491.67) + M_s u_s + M_w u_w$$

for superheated,

$$U_{as} = M_a C_v (T_{as} - 491.67) + M_s u_s$$

- d. Determine temperature by comparing  $U_{as}$  with actual internal energy
- e. Calculate pressure from the determined temperature.

for two-phase,

$$P = \frac{M_a R_a T}{V} + \frac{M_s R_s T}{V} \left[ 1 + \frac{M_s}{V} B(T) \right]$$

for superheated,

$$P = \frac{M_a R_a T}{V} + \frac{M_s R_s T}{V_s}$$

where  $V_s$  is the volume of the steam flow.

Here, step *d* and *e* are performed iteratively.

- iii) Flow rates are calculated on the basis of the existing pressure differential between subcompartments.

$$\frac{L}{A} \frac{d\dot{m}}{dt} = \Delta P - \frac{K}{A^2} \frac{\dot{m}^3}{2\rho}$$

- iv) Mass and energy are readjusted in each subcompartment and new thermodynamic conditions are determined.

##### 2) Sensitivity for Time Step

In order to observe the variation of calculated values for the short term subcompartment analysis of V. 42, V. 43 and V. 44 experiments accor-

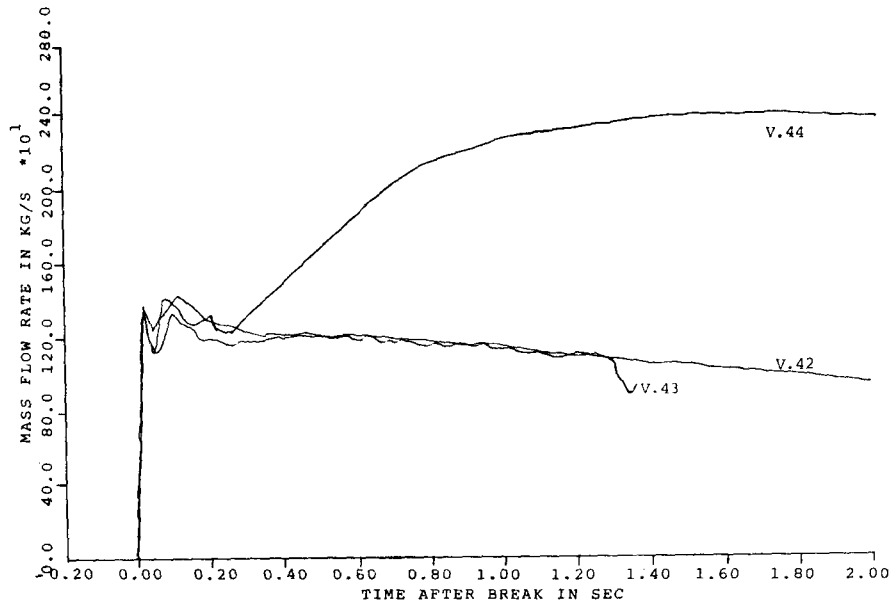


Fig. 3. Mass Flow Rate vs Time After Break

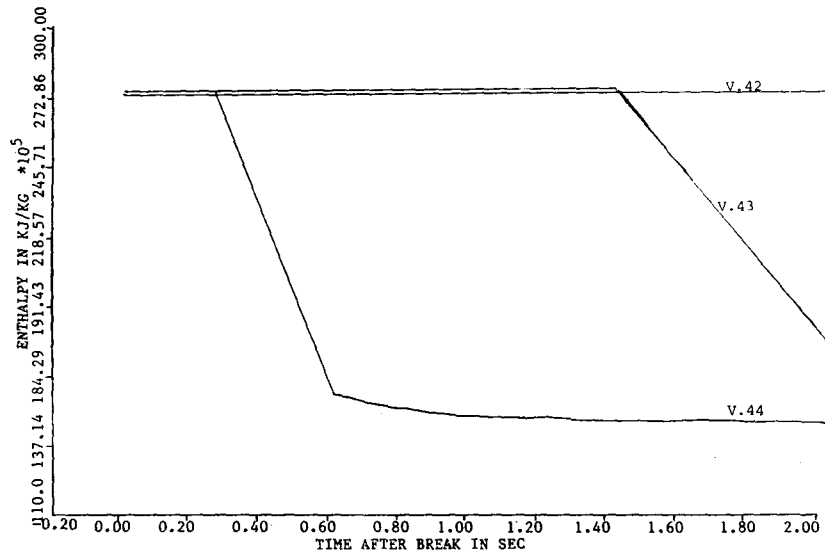


Fig. 4. Enthalpy vs Time After Break

ding to time step size, similar calculations are performed repeatedly according to time step sizes; 0.01, 0.0075, 0.005, 0.0025, 0.001 sec for the three tests, which are selected in consideration of blowdown rates shown in Figure 3 and Figure 4. They show that the differences of calculated values are insignificant. The parameters variations due to time step size are well agreed within 0.2% on the basis of 0.005 sec time step. Therefore the analysis will be carried out with time step size of 0.005 sec.

## V. Results and Discussion

In the subcompartment analysis, the largest pressure and pressure gradient appear between the break compartment to the adjacent compartments. Hence the volumes related with junction 3, 4 and 5 are mainly selected for the comparison between calculated and measured values of interests in consideration of the degree of geometric complexity. The pressure difference and the absolute pressure calculated by using the suggested head loss coefficient expressions, equation (3) and (4), are illustrated in Figure 6 to

Figure 11. The calculated values are systematically higher in the order of equations (3), (4) and (5). These usually overestimate the measured values for V. 42, V. 43 tests and underestimate for test V. 44. Generally the pre-test best estimate calculations of pressure differences for V. 42, V. 43 and V. 44 tests show tendencies to underestimate the measured values. For example, the pressure and pressure difference calculated by CONTEMPT-4 code with the head loss coefficient of 1.6 and 10% liquid deposition are compared with experimental values in Figure 5 along with the results of COMPARE code with the same head loss coefficient of 1.6 and no liquid deposition. Thus it may be considered that head loss coefficient has been underestimated. As shown in Figure 3 and Figure 4, the blowdown rate and quality are similar to those at about 1.4 sec for V. 42 and V. 43 tests. The changes of effective density and flow rate are regarded as very small but in V. 43 is smaller than in V. 42. But pressure differences for V. 43 test are clearly lower than for V. 42. Therefore it is concluded that the flow resistance is lower and the break flow distribution

by the movement of the impingement plate causes the difference. As shown in the figures, more overestimation for V. 43 than for V. 42 is attributed to the relatively diminished measured values caused by further movement of impingement plate from the break nozzle and lower total blowdown energy. So it may be thought

the location and the geometry of pipe break and the geometry in the immediate vicinity of the break is important for the calculation of the values of interest in the subcompartment analysis. Unfortunately, it can not be explicitly represented by the lumped parameter models. The calculated results by using Equation (3) show generally

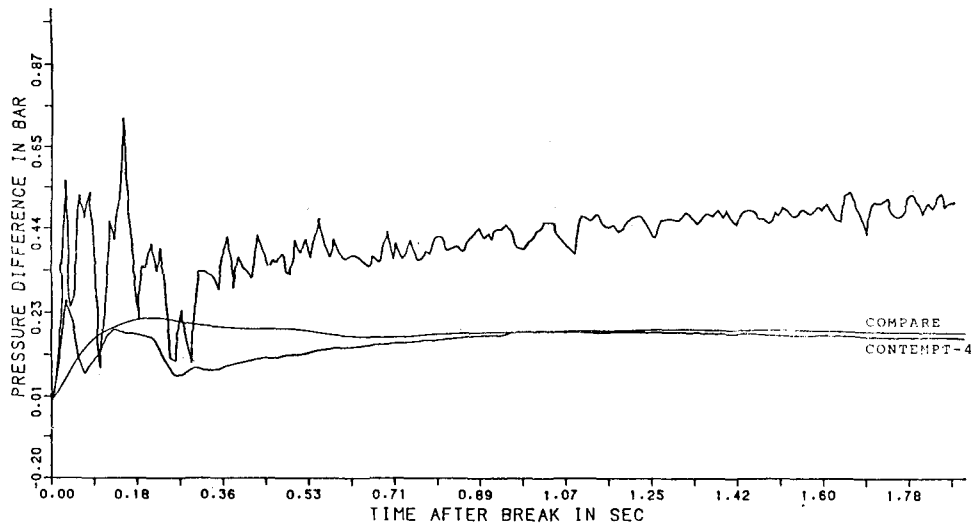


Fig. 5. Calculated and Measured  $\Delta P$  Across Junction 3 For V. 44 Test

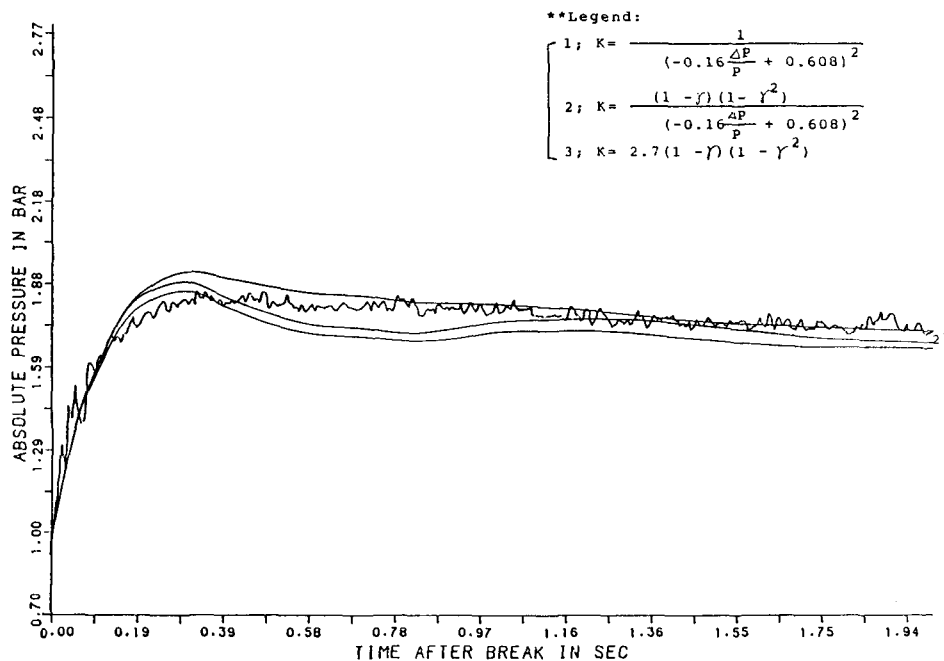


Fig. 6. Calculated and Measured Pressures in Break Compartment For V. 42 Test

better agreement with experiments through Figure 6 to Figure 11 except Figure 11. As shown in Figure 11, the difference between the experimental and calculated values is larger for junction 3, which has the most complex geometry. On the other hand, values calculated by using equation (4) are more closed to the measured values, but it is not the case for the

other junctions. This is an explanation of the necessity for introducing geometric factor into equation (3) for very complex flow openings. In practice, A and B are not constant in the equation (3), expressed as the form of  $(A \frac{\Delta P}{P} + B)^{-2}$ , but dependent on the geometric shape. And another consideration is that the junctions are nonconcentric orifice type. As the junctions

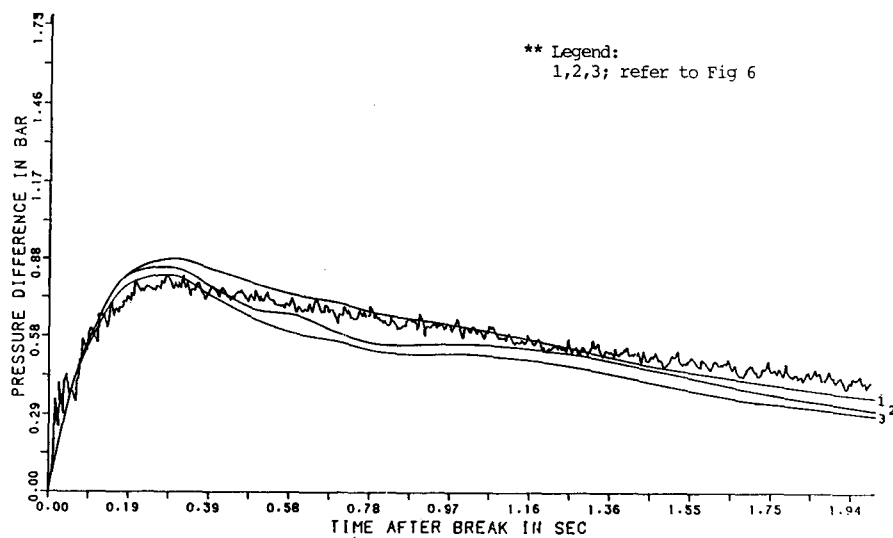


Fig. 7. Calculated and Measured  $\Delta P$  Across Junction 5 For V. 42 Test

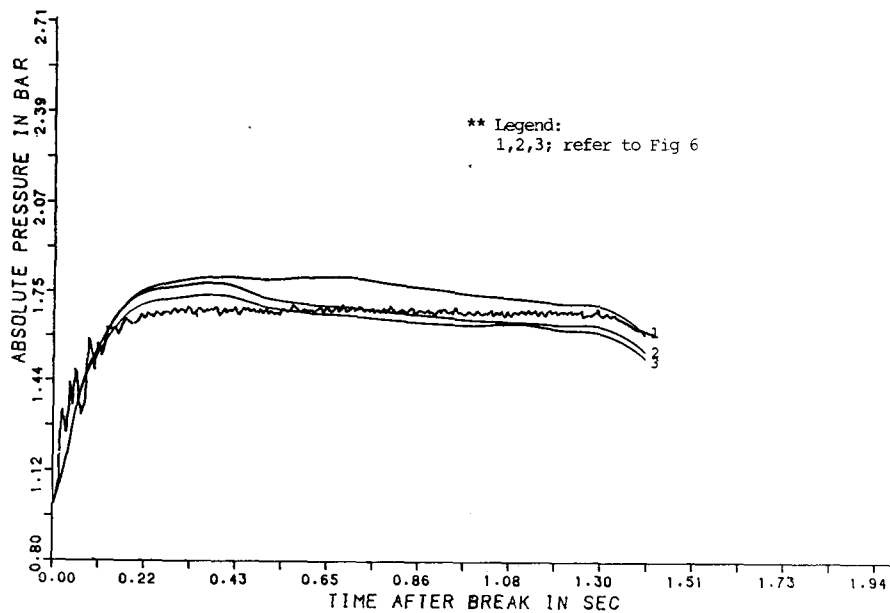


Fig. 8. Calculated and Measured Pressures in Break Compartment For V. 43 Test



are considered as nonconcentric and flow diameter increases, the head loss coefficient tends to increase. For the above calculations, liquid deposition in the subcompartment is not taken into account, but physical observation and experimental evidence suggest that liquid droplet deposition does occur. This alters the averaged density in a subcompartment and leads to lower

pressure difference than in the case of no liquid deposition. Particularly, it is expected that substantial liquid deposition will occur due to flow resistance in passing through very complex flow openings. Therefore, if droplet deposition is considered in the calculation of HDR tests, the overestimated values are expected to approach the measured values for V.42 and V.43 tests.

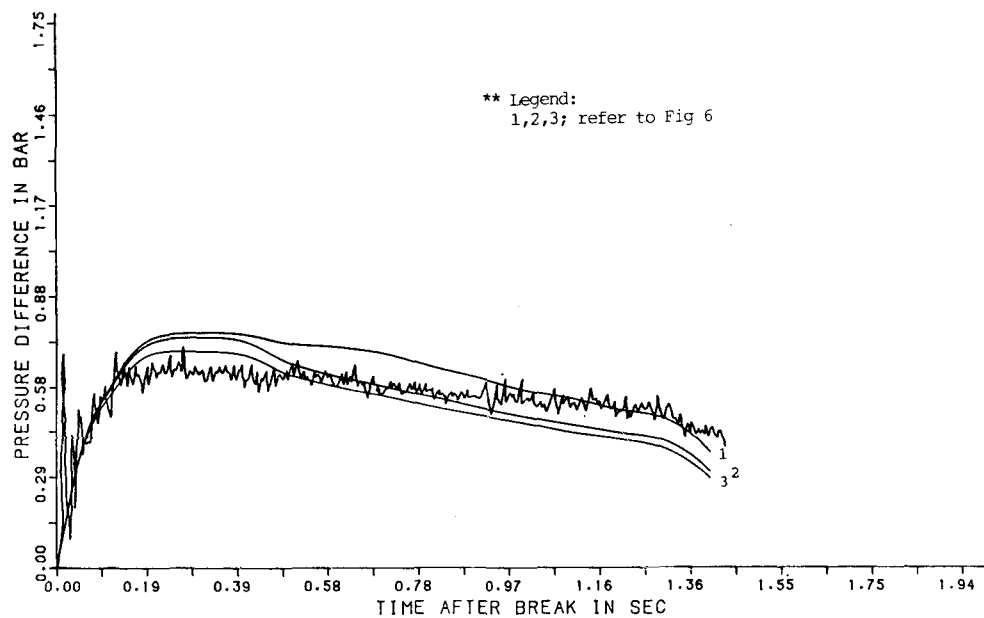


Fig. 9. Calculated and Measured  $\Delta P$  Across Junction 4 For V. 43 Test

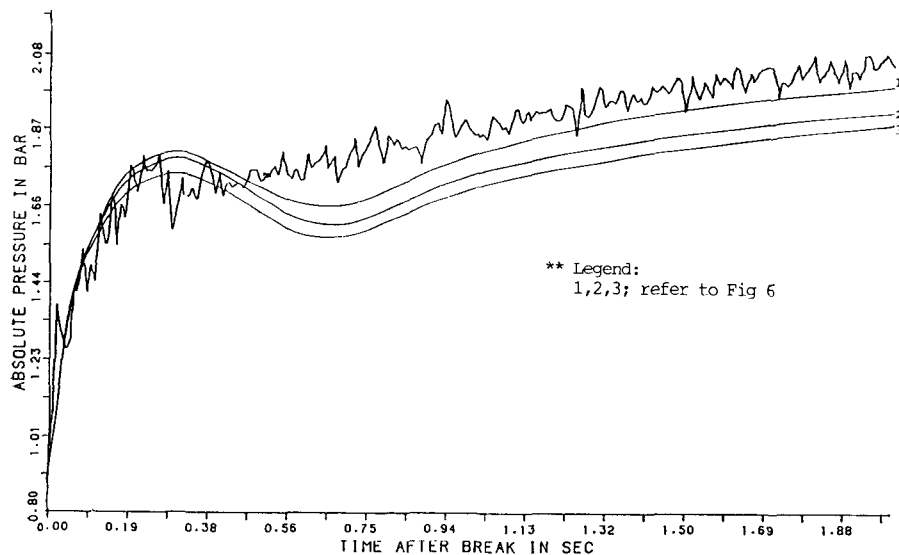


Fig. 10. Calculated and Measured Pressures in Break Compartment For V. 44 Test

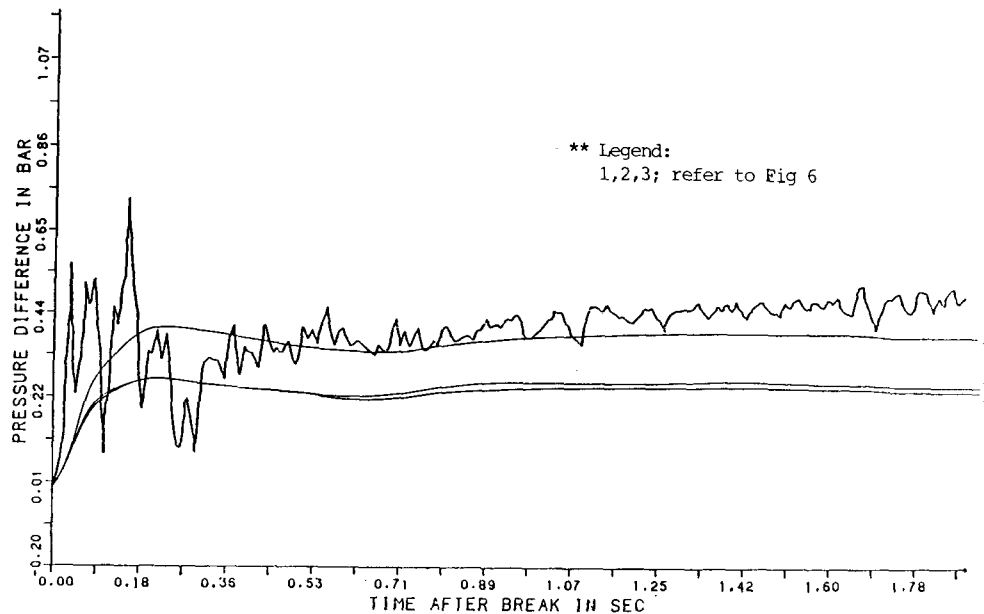


Fig. 11. Calculated and Measured  $\Delta P$  Across Junction 3 For V. 44 Test

But for V. 44 test more underestimation is expected. As illustrated in Figure 3 and Figure 4, the steam flows out up to about 1.3sec for V. 42 and V. 43 tests when two-phase flow starts, the influence of the liquid deposition increases substantially and the effect of compressibility in equation (3) will be smaller as quality decreases. Thus equation (3) and (4) also require the consideration for liquid deposition model.

## VI. Conclusion

As shown in the results, the pressure and pressure differences calculated by using COMPARE code with revised model come to close to the measured values for V. 42 tests, but overestimate the experimental values for V. 43 and underestimate for V. 44 tests. These trends may lead that the suggested head loss coefficient must be further modified for the very complex vent and low quality conditions, for instance, introducing proper shape factor and/or two-phase

multiplier. Since the pressure difference is closely related to the head loss coefficient, flow rate, effective flow density and flow area ratio, it may be considered difficult to obtain satisfactory results with the modification of head loss coefficient only. Among those parameters the effective density turns out to have a large influence on the calculation of pressure difference. Liquid deposition, which U.S. NRC guideline does not allow for the subcompartment analysis for the conservatism, however, in reality reduces the compartment density remarkably. Thus consideration of suspended water transport is suggested for more realistic and precise subcompartment analysis.

## References

1. K. Almenas, U.C. Lee and S. Traifors, "Scaling Methodology for Subcompartment Analysis," Fifth International Meeting on Thermal Nuclear Reactor Safety, Karlsruhe, FRG. on Sep. 9-13 (1984).

2. K. Almenas, "Comparison of Experimental and Calculated Pressure Differences in the HDR Containment," PHDR Arbeitsbericht Nr. 3. 388/83 (1983)
3. S.J. Hong, "COMPARE CODE User's Manual," KOPEC (1984)
4. Idel'chik, I.E., "Handbook of Hydraulic Resistance," ACE-TR-6630 (1966)
5. Howard, S.B., "Fluid Meters; Their Theory and Application," 4th ed. A.S.M.E. (1837)
6. S. Traifors, "Liquid Suspension in Subcompartment Analysis; Investigation of its Treatment and a New Approach," Ph.D. thesis in University of Maryland (1982)
7. Gido, R.G. Gilbert, J.S. and Tinkler, C.G., "Subcompartment Analysis Procedure," NUREG/CR-1199 (1979)
8. E. Buckingham, "Notes on Some Recently Published Experiments on Orifice Meters," A.S.M.E. FEB. (1956)
9. F. Kreith, R. Eisenstadt, "Pressure Drop and Flow Characteristics of Short Capillary Tubes at Low Reynolds Numbers," A.S.M.E. July (1957)
10. R.M. Olson, "Essentials of Engineering Fluid Mechanics," 4th ed. (1980)
11. T.C. Cheng et al., "CONTEMPT-4/MOD 3 Manual", TREE-NUREG/CR-2558 (1982)
12. Versuchsprotokoll Blowdown-Versuch V-42 (19/08/82) PHDR 3.32/82
13. Versuchsprotokoll Blowdown-Versuch V-43 (09/8/82) PHDR 3.329/82
14. Versuchsprotokoll Blowdown-Versuch V-44 (07/10/82) PHDR 3.376/83